

Linewidth measurement of Littrow structure semiconductor laser with improved methods

Wu Zhou, Kin Man Chong, Hong Guo *

CREAM Group, School of Electronics Engineering & Computer Science, Peking University, Beijing 100871, PR China

Received 1 September 2007; received in revised form 26 March 2008; accepted 27 March 2008

Available online 1 April 2008

Communicated by R. Wu

Abstract

In this Letter, the frequency noise spectrum is analyzed in the experiment of the laser linewidth measurement. The power spectrum of three most widely used laser linewidth measurement methods, i.e., the heterodyne measurement, the self-homodyne measurement and the self-heterodyne measurement, are restudied both theoretically and experimentally. A scheme adopting an avalanche photodetector (APD) in the delayed self-heterodyne (DSHT) method is proposed, and an indirect determined result is given.

Crown Copyright © 2008 Published by Elsevier B.V. All rights reserved.

OCIS: 300.3700; 030.1640; 140.5960

Keywords: Semiconductor laser; Frequency noise; Linewidth; Homodyne; Heterodyne

1. Introduction

With great interests in coherent optical communication, optical precision metrology and high-resolution spectroscopy, much effort is being done to develop semiconductor lasers with narrow linewidth. Therefore, the linewidth measurements of the semiconductor lasers becomes more and more important. So far, some methods have been proposed and used for linewidth determination of the diode lasers [1–4]. The theories used in the laser linewidth measurement are closely related to those in the laser spectrum, i.e., the well-known Schawlow–Townes linewidth formula, which is later revised and generalized by Henry and Fleming [5–7]. In the previous work [8], it is complicated to get the photocurrent spectrum, and the result often includes DC part, which introduces the additional frequency modulation (FM) noise and thus broadens the spectrum linewidth of the photocurrent [9]. Hence, a general analysis for FM noise and further, an effective method for reducing the FM noise is needed.

In the following work of laser linewidth measurement, three methods are adopted, they are, the beat of two lasers (BTL), the delayed self-homodyne (DSHO) and the delayed self-heterodyne (DSHT), the schematic setups of which are illustrated in Fig. 1: two external cavity diode lasers (ECDL) with the same Littrow structures are composed of a diode laser ($\lambda = 852$ nm, max power 500 mW), a collimating objective, a reflective grating and an output mirror. The external grating feedback configuration of the Littrow structure is expected to narrow the linewidth of the diode laser down to hundreds kilohertz scale. The ECDL is prepared to operate in the single mode for the convenience of measurement and analysis.

2. FM noise spectrum

The optical field in ECDL can be modeled as a quasi-monochromatic field with random phase fluctuation and slowly varying amplitude, i.e.,

$$E(t) = E_0[1 + E_\delta(t)]e^{i[\omega_0 t + \phi(t)]}, \quad (1)$$

where ω_0 , $E_\delta(t)$ and $\phi(t)$ are, respectively, the central frequency, the time dependent magnitude and the phase of the field.

* Corresponding author. Tel.: +86 10 6275 7035; fax: +86 10 6275 3208.
E-mail address: hongguo@pku.edu.cn (H. Guo).

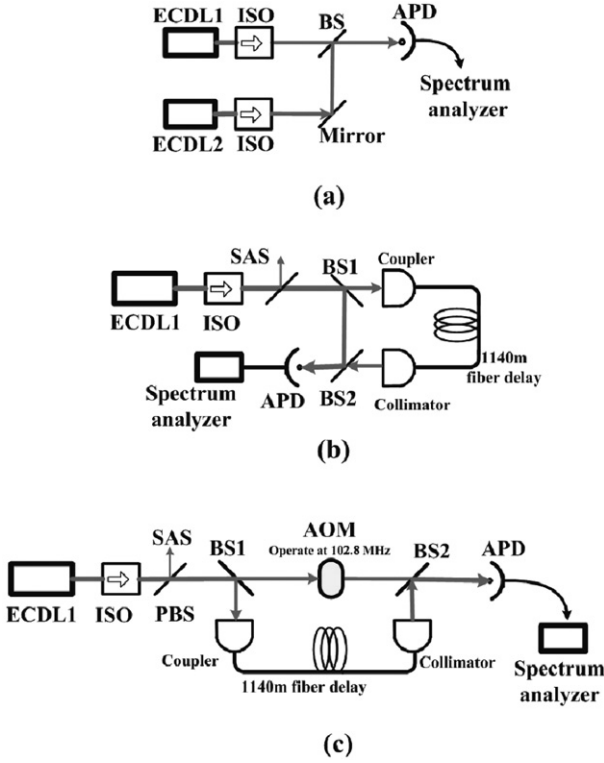


Fig. 1. Experiment setup of three linewidth measurement methods. (a) beat of two lasers (BTL); (b) delayed self-homodyne (DSHO); (c) delayed self-heterodyne (DSHT); EC DL: external cavity diode laser; ISO: optical isolator; SAS: saturation-absorption spectrometer; AOM: acousto-optic modulator; APD: avalanche photo-detector.

Using Maxwell's equations and carrier density $[n(t)]$ function, motion equations of $E_\delta(t)$, $\phi(t)$ and $n(t)$ are described as (see Appendix A):

$$\dot{E}_\delta + \frac{\xi_r}{\eta^2} \dot{n} - \frac{\omega_0 \xi_i}{2\eta^2} n = \frac{\Delta_i}{2\omega_0 E_0}, \quad (2)$$

$$\dot{\phi} + \frac{\xi_i}{\eta^2} \dot{n} + \frac{\omega_0 \xi_r}{2\eta^2} n = -\frac{\Delta_r}{2\omega_0 E_0}, \quad (3)$$

$$\dot{n} + \frac{n}{\tau_R} + \frac{2\eta^2 \omega_R^2}{\omega_0 \xi_i} E_\delta = \vartheta, \quad (4)$$

where η is the nonresonant index, ξ_r and ξ_i are the first order coefficients of the Taylor expansions of the real and imaginary parts of the refractive index, i.e., χ_r and χ_i , near steady state n_0 , Δ (the subscript of Δ , r and i , indicates its real and imaginary parts, respectively) and ϑ are the Langevin noise terms due, respectively, to the spontaneous radiation and thermal motion of carriers. Therefore, the frequency spectrum can be calculated using Wiener-Khinchine theorem through auto-correlation function $\langle \Delta\omega(t+\tau)\Delta\omega(t) \rangle = \langle \dot{\phi}(t+\tau)\dot{\phi}(t) \rangle$:

$$W_f(\omega) = \frac{G}{4\omega_0^2 E_0^2} + \left[\frac{G\alpha^2 \omega_R^4}{4\omega_0^2 E_0^2} + \frac{\omega_0^2 \xi_r^2 G_2 \omega^2}{4} \right] / [(\omega^2 - \omega_R^2)^2 + \omega^2 / \tau_R^2], \quad (5)$$

where G and G_2 are the coefficients of the Langevin force relations, ω_R is the frequency caused by the relaxation oscillation (fluctuation) of the carrier density, and τ_R is the damping time

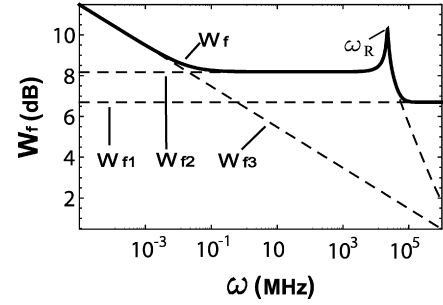


Fig. 2. Frequency noise spectrum W_f [Eq. (5)] at photon density $p_0 = 1 \times 10^{14} \text{ cm}^{-3}$ [15]. $W_f = W_{f1} + W_{f2} + W_{f3}$, W_{f1} : white noise, W_{f3} : $1/f$ noise, W_{f2} : residual spectrum.

(see Appendix B), and $\alpha = \xi_r / \xi_i$ is known as the linewidth enhancement factor.

It can be found, from Eq. (5), that the FM noise spectrum is mainly composed of two parts: the white noise (W_{f1}) caused by the spontaneous emission, and the frequency spectrum (W_{f2}) centered in ω_R originated from the relaxation oscillation. Besides, according to experimental results, another low frequency noise source W_{f3} , known as $1/f$ noise, is added to Eq. (5), with a constant factor K [10]. It will be seen in the following that K is the measurement of the $1/f$ noise influence, and is an important parameter to determine the power spectrum linewidth. Thus, the spectrum is now expressed with three parts:

$$W_f(\omega) = W_{f1} + W_{f2} + W_{f3}, \quad (6)$$

$$W_{f1} = W_0 = G/4\omega_0^2 E_0^2, \quad (7)$$

$$W_{f2} = \left[\frac{G\alpha^2 \omega_R^4}{4\omega_0^2 E_0^2} + \frac{\omega_0^2 \xi_r^2 G_2 \omega^2}{4} \right] / [(\omega^2 - \omega_R^2)^2 + \omega^2 / \tau_R^2], \quad (8)$$

$$W_{f3} = K/|\omega|. \quad (9)$$

The frequency spectrum W_f is plotted in Fig. 2, using parameters [see Appendices A and B, Eqs. (A.7), (A.11), (A.12), (B.7), (B.9), for details] with the typical values of $\alpha^2 = 30$, $g = 0.5 \times 10^{12} \text{ s}^{-1}$, $dg/dn = 10^{-6} \text{ cm}^3 \text{ s}^{-1}$, $\tau_s = 1 \text{ ns}$, $V_c = V = 3 \times 10^{-10} \text{ cm}^3$, $n_0 = 10^{18} \text{ cm}^{-3}$, $\omega_0 = 2.2 \times 10^{15} \text{ rad s}^{-1}$ (852 nm), and $E_{cv} = 1.6E_{vc}$ [6].

It can be seen from Fig. 2 that W_{f1} and W_{f2} is mostly flat before ω_R (\sim several GHz). In the case of our DSHO and DSHT measurement methods, the highest central frequency is ω_A (102.8 MHz) which satisfies $\omega_A \ll \omega_R$. Therefore, the contribution of W_{f1} and W_{f2} is approximated as:

$$W_{f0}(\omega)|_{\omega \ll \omega_R} = W_{f1} + W_{f2} \approx W_0(1 + \alpha^2), \quad (10)$$

where $W_0 = W_{f1}$ is the original white noise term. In the following, the analysis will be made based on the above assumption. It then follows that the total FM noise spectrum is:

$$W_f(\omega) \approx W_{f0} + W_{f3} = W_0(1 + \alpha^2) + \frac{K}{|\omega|}. \quad (11)$$

3. Power spectrum

In the following, we show the experiment results of the power spectrum using the spectrum analyzer. Due to different optical field detected in different measurement setups of our experiments, power densities are derived below according to three methods mentioned above.

The BTL method is illustrated in Fig. 1(a). The beat signal is detected directly by using a fast avalanche photo-detector (APD, Hamamatsu5658, 50 kHz–1 GHz), and the power spectrum is analyzed by a spectrum analyzer (HP8568). The total electric field is simply the sum of the two lasers, with two different center frequencies ω_{01} and ω_{02} . Then, the detected photocurrent is given by $I_b(t) = 2D_0E_{01}E_{02} \cos[\Delta\omega_0 t + \phi_1(t) - \phi_2(t)]$, where $\Delta\omega_0 = \omega_{01} - \omega_{02} = \Delta\lambda \cdot 2\pi c/\lambda^2$, and D_0 is the gain coefficient. Since we used the APD in the experiment, only the AC component is included here. As what Wiener-Khinchine theorem predicts, the spectral density of $I_b(t)$ is simply the Fourier transform of its autocorrelation function $R_{I_b}(\tau) = \langle I_b(t + \tau)I_b(t) \rangle$, i.e.,

$$S_b(\omega) = S_{b0} \frac{1/\tau_c}{(1/\tau_c)^2 + (\omega \pm \Delta\omega_0)^2}, \quad (12)$$

where $S_{b0} = 4D_0^2E_{01}^2E_{02}^2$ is a constant depending on the detector and the intensity of the laser beams, $1/\tau_c = 1/\tau_{c1} + 1/\tau_{c2}$ is the total coherence time. In deriving Eq. (12), $\langle \exp[i\Delta\phi(t)] \rangle = \langle \exp[-\frac{1}{2}\langle \Delta\phi(t)^2 \rangle] \rangle$ is used, where $\Delta\phi(t) = \phi_1(t) - \phi_2(t)$ [11]. From Eq. (12), the linewidth of the photocurrent is simply the sum of those of two independent lasers.

The center wavelength of ECDL is about 852 nm, $\Delta\lambda = 1$ nm ($\Delta\omega_0 \approx 2.6$ THz), which is out of the band of APD. Therefore, BTL method is not suitable in our experiment setup. In deriving Eq. (12), it is reasonable for us to assume that the AM noise is negligible because $E_\delta(t)$ is slowly varying compared with the laser frequency, and that the spectral width is caused mainly by the FM noise. This assumption is used throughout this Letter.

DSHO configuration is shown in Fig. 1(b). The laser beam is separated into two paths by a 50/50 beam splitter after frequency stabilization. One of them is delayed by a 1.14 km single mode fiber, and then beat with the other through a 50/50 beam splitter. The beat signal can be written as $E_O(t) = E_0 \exp[i(\omega_0 t + \phi(t))] + E_0 \exp[i(\omega_0(t + \tau_d) + \phi(t + \tau_d))]$, where τ_d is the fiber caused delay time. It is easy to deduce the photocurrent using $I(t) = |E(t)|^2$, and further, the photocurrent autocorrelation function and the spectrum (see Appendix C):

$$R_I(\tau) = I_0 \exp \left[-\frac{4}{\pi} \int_{-\infty}^{\infty} W_f(\omega) \times \frac{(1 - \cos \omega\tau)(1 - \cos \omega\tau_d)}{\omega^2} d\omega \right], \quad (13)$$

$$S_{IO}(\omega) = I_0 \mathfrak{F}[R_I(\tau)] = I_0 \mathfrak{F}[R_{I0}(\tau) \times R_{I3}(\tau)] = I_0 S_{f0} * S_{f3}, \quad (14)$$

where \mathfrak{F} denotes the Fourier transform, R_{I0} and R_{I3} are, respectively, the autocorrelation functions corresponding to the

enhanced white noise induced power density S_{f0} , the $1/f$ noise induced power density S_{f3} , and $*$ denotes the convolution. R_{I0} and R_{I3} can be obtained by substituting W_{f0} and W_{f3} into Eq. (13), and using the relations:

$$\int_0^{\infty} \frac{\cos(\omega\tau)}{\omega^{3+\theta}} d\omega = \Gamma(-2 - \theta) Re(i\tau)^{2+\theta}, \quad (15)$$

$$\int_0^{\infty} \frac{1}{\omega^{3+\theta}} d\omega = \lim_{\lambda \rightarrow 0} \lambda^{2+\theta} \Gamma(-2 - \theta), \quad (16)$$

which gives

$$R_{I0}(\tau) = \begin{cases} e^{-W_0(1+\alpha^2)|\tau|}, & |\tau| < \tau_d, \\ e^{-W_0(1+\alpha^2)\tau_d}, & |\tau| \geq \tau_d, \end{cases} \quad (17)$$

$$S_{f0}(\omega) = \frac{2W_0(1+\alpha^2)}{[W_0(1+\alpha^2)]^2 + \omega^2} \times \left\{ 1 - e^{-W_0(1+\alpha^2)\tau_d} \times \left[\cos \omega\tau_d + W_0(1+\alpha^2) \frac{\sin \omega\tau_d}{\omega} \right] \right\}, \quad (18)$$

$$R_{I3}(\tau) = |\tau + \tau_d|^{-K|\tau + \tau_d|^2/2\pi} |\tau - \tau_d|^{-K|\tau - \tau_d|^2/2\pi} \times |\tau|^{K\tau^2/\pi} |\tau_d|^{K\tau_d^2/\pi}, \quad (19)$$

$$S_{f3}(\omega) = \mathfrak{F}[R_{I3}(\tau)]. \quad (20)$$

The DSHO method seems to be a good method in theory, but it can be observed from the experiment that some additional low frequency noises, which are introduced by mechanical devices, detector and analyzer, are included. The zero input analyzer's spectrum has a sharp pulse centered in zero frequency with several kilohertz width. Hence, the power spectrum is buried in the low frequency noise near zero point. Therefore, the DSHT method is proposed, in order to avoid these kinds of noises. The experiment setup is illustrated in Fig. 1(c) by employing an acousto-optic modulator (AOM) which operates at $\omega_A = 102.8$ MHz in the short arm of the DSHO setup. The laser field then becomes $E_E(t) = E_0 \exp\{i[(\omega_0 + \Omega)t + \phi(t)]\} + E_0 \exp[i(\omega_0(t + \tau_d) + \phi(t + \tau_d))]$, therefore, the shifted photocurrent autocorrelation function and the spectrum are:

$$R_I(\tau) = I_0 \cos(\omega_A \tau) R_{I0}(\tau) R_{I3}(\tau), \quad (21)$$

$$S_E(\omega) = I_0 \mathfrak{F}[R_I(\tau)] = I_0 \mathfrak{F}[\cos(\omega_A \tau) R_{I0}(\tau) \times R_{I3}(\tau)]. \quad (22)$$

4. Results and conclusion

The BTL method spectrum [i.e., S_b , Eq. (12)], the analytical Fourier transform of R_{I0} [i.e., S_{f0} , Eq. (18), white noise], the fast Fourier transform of R_{I3} [i.e., S_{f3} , Eq. (20), $1/f$ noise], and the fast Fourier transform of R_I [i.e., total spectrum S_{IO} , Eq. (14)] are plotted in Figs. 3-5, respectively. In Fig. 3, compared with $S_b(\omega)$, S_{f0} has an exponential decay term, which is due to the self-correlation of the laser field. It indicates that the power spectrum of the enhanced white noise induced spectrum

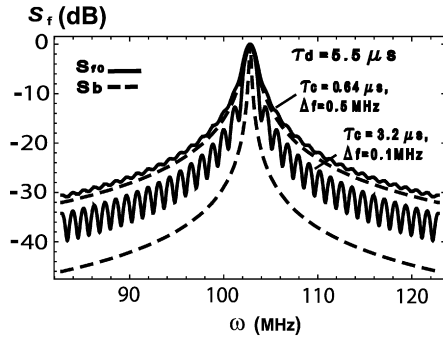


Fig. 3. Power spectrum S_{f0} introduced by white noise alone [Eq. (18)]. Solid lines show two cases for $\tau_c = 0.64 \mu\text{s}$, $3.2 \mu\text{s}$. The fiber delay time is fixed at $5.5 \mu\text{s}$. Dashed lines are the BTL method spectrum S_b [Eq. (12)] with the same parameters. It shows that when τ_c gets bigger, the difference between S_{f0} and S_b gets bigger, and further, the oscillation of S_{f0} gets more evident.

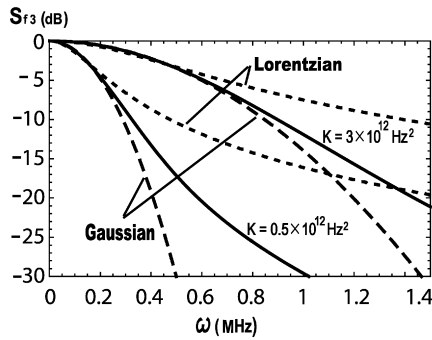


Fig. 4. Power spectrum introduced by $1/f$ noise alone (i.e., S_{f3}). Solid lines are the fast Fourier transform of R_{f3} [Eq. (19)], with different factors $K = 3 \times 10^{12} \text{Hz}^2$, $0.5 \times 10^{12} \text{Hz}^2$. Dashed and dotted lines are, respectively, Gaussian and Lorentzian lineshapes with the same 3 dB linewidth as S_{f3} .

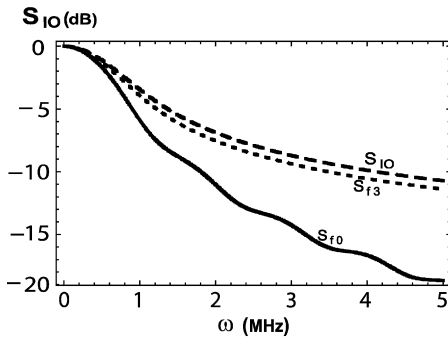


Fig. 5. Total power spectrum S_{I0} in DSHO method, which is the convolution of S_{f0} (Fig. 3) and S_{f3} (Fig. 4) using Eq. (14). Parameters are: $\tau_c = 0.64 \mu\text{s}$, $K = 3 \times 10^{12} \text{Hz}^2$. It can be seen that after the convolution the total spectrum gets flat in high frequency region.

becomes strictly Lorentzian as the delay time increases. This can be explained as the decorrelation of the laser field after long distance delay. Fig. 4 shows a numerical plot of S_{f3} , which is the $1/f$ noise. Careful analysis in expression of R_{f3} found its Gaussian approximation in low frequency region. The dashed Gaussian lineshapes in Fig. 4 are plotted with the same FWHM (full width half maximum) according to S_{f3} . Then, considering both white noise and $1/f$ noise, in general noise analysis, their convolution is numerically presented in Fig. 5. It is obvious that

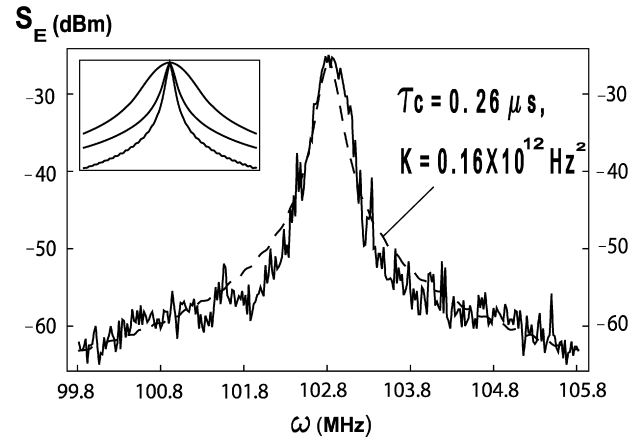


Fig. 6. Fit of experimental DSHT power spectrum using indirect method. The dashed line is the numerical approximation of power spectrum S_E [i.e., Eq. (22)]. Parameters used to fit the data are: $\tau_c = 0.26 \mu\text{s}$, $K = 0.16 \times 10^{12} \text{Hz}^2$. The inset figure is the fit function Eq. (22). Upper: $\tau_c = 0.64 \mu\text{s}$, $K = 3 \times 10^{12} \text{Hz}^2$, middle: $\tau_c = 0.64 \mu\text{s}$, $K = 0.16 \times 10^{12} \text{Hz}^2$, low: $\tau_c = 0.26 \mu\text{s}$, $K = 0.16 \times 10^{12} \text{Hz}^2$. τ_c and K determine the wings and the center part of the lineshape.

the $1/f$ noise broadens the power spectrum S_{I0} through the convolution of S_{f0} and S_{f3} .

Therefore, when $\tau_d \gg \tau_c$, S_{f0} becomes the Lorentzian lineshape. On the other hand, S_{f3} tends to be a Gaussian lineshape in low frequency band (Fig. 4). A convolution of them leads to a Voigt lineshape in $S_E(\omega)$ [Eq. (22)]. Furthermore, careful analysis indicates that $S_{f0}(\omega)$, $S_{f3}(\omega)$, $S_{I0}(\omega)$ and $S_E(\omega)$ are functions of ω with independent parameters τ_d , τ_c (linewidth), K and the output power. In our DSHT method, $\tau_d \approx 5.5 \mu\text{s}$ and the output power is 20 mW. The numerical simulations are made to fit the experimental data while changing the other two parameters τ_c and K . Therefore, the laser linewidth can be determined indirectly under short fiber delay. The indirect data fit method is applied and the results are shown in Fig. 6, with parameters $\tau_c = 1/\pi \Delta f = 1/[\pi S_0(1 + \alpha^2)] = 0.26 \mu\text{s}$, $0.64 \mu\text{s}$, $K = 0.16 \times 10^{12} \text{Hz}^2$, $3 \times 10^{12} \text{Hz}^2$, which show that the laser linewidth is about 200 kHz. The result shows a good match with theory given above. It is found that τ_c controls the wings and K controls the center of the lineshape.

The noise levels of the three methods are different: for BTL, the noise originates from two independent lasers and so the total noise is simply the sum of that of the two lasers. For DSHO, only one laser is used, the noise from the lasers is around one half of that of BTL. However, zero point noise exists in the background of the photocurrent due to the spectrum analyzer. For DSHT, the advantages of DSHO are kept while the low frequency noises are kept outside of the beat frequency and so, the noise is the least among the three methods (Fig. 6).

In conclusion, we derive formula to determine the linewidth of the semiconductor lasers, which has the advantages of clarity and feasibility for the experiment. The frequency noise is analyzed in detail. Further, an improvement in the detection has been made and an indirect approach of photocurrent spectrum is obtained. Using the theory and methods proposed in this Letter, the experiment is conducted, and the experiment results

coincide with those given by theories. But still, there are some problems to be explored, such as the sidemodes influence, the fiber dispersion, etc., [12,13]. Since our laser runs in CW single mode and the fiber is around 1 km long, these influence can be ignored. Provided that these problems are solved, the measurement of the laser linewidth would be easier and more accurate.

Acknowledgements

This work is supported by the National Natural Science Foundation of China (Grant No. 10474004), and DAAD exchange program: D/05/06972 Projektbezogener Personenaustausch mit China (Germany/China Joint Research Program).

Appendix A. Motion equations

We start from Maxwell's equations:

$$\nabla \times \vec{E}(\vec{r}, t) = -\mu \partial_t \vec{H}(\vec{r}, t), \quad (\text{A.1})$$

$$\nabla \times \vec{H}(\vec{r}, t) = \sigma \vec{E}(\vec{r}, t) + \partial_t [\epsilon \vec{E}(\vec{r}, t) + \vec{P}(\vec{r}, t)] + \partial_t \vec{s}(\vec{r}, t), \quad (\text{A.2})$$

where μ is the magnetic permeability, σ is the medium conductivity, $\epsilon = \epsilon_0 \eta^2$ is the nonresonant dielectric constant and η is the nonresonant medium index, $\vec{P}(\vec{r}, t)$ and $\vec{s}(\vec{r}, t)$ are the induced polarization caused by the stimulated and the spontaneous transitions, respectively. We treat $\vec{s}(\vec{r}, t)$ as a fluctuation noise due to the random phase of the spontaneous emission. The polarization can be written as $\vec{P}(\vec{r}, t) = \epsilon_0 \chi(n) \vec{P}(\vec{r}, t)$, where $\chi = \chi_r + i \chi_i$, is the susceptibility on the medium, and is dependent of the carrier density n .

Using the expansions as follows:

$$\vec{E}(\vec{r}, t) = \sum_n E_n(t) \vec{e}_n(\vec{r}), \quad (\text{A.3})$$

$$\vec{P}(\vec{r}, t) = \sum_n P_n(t) \vec{e}_n(\vec{r}), \quad (\text{A.4})$$

$$\vec{s}(\vec{r}, t) = \sum_n s_n(t) \vec{e}_n(\vec{r}), \quad (\text{A.5})$$

one yields

$$\begin{aligned} \frac{d^2}{dt^2} \left[\left(1 + \frac{\chi(n)}{\eta^2} \right) E_n \right] + \frac{1}{\tau_p} \frac{d}{dt} E_n + \omega_n^2 E_n \\ = -\frac{1}{\epsilon_0} \frac{d^2}{dt^2} s_n = \Delta e^{i\omega_0 t}, \end{aligned} \quad (\text{A.6})$$

where $\tau_p = \epsilon_0/\sigma$ is the photon lifetime, ω_n is the resonant frequency of the n th mode, ω_0 is the laser frequency, Δ is the slowly varying term of $\frac{d^2}{dt^2} s_n(t)$, which is treated as a Langevin noise source due to classical result [14] and "white" nature of the spontaneous emission.

In addition, the carrier density n can be depicted by rate equation as

$$\dot{n} + g(n)p + \frac{n}{\tau_s} = R + \vartheta, \quad (\text{A.7})$$

where $g(n) = \omega_0 \chi_i / \eta^2$ is the gain, $p = \epsilon_0 \eta^2 |E|^2 / 2\hbar \omega_0$ is the photon density, τ_s is the spontaneous lifetime, R is the pumping rate and ϑ is the noise term treated as Langevin noise.

Considering single mode case and substituting $E(t)$ [Eq. (1)] into Eqs. (A.6) and (A.7) yields:

$$\dot{E}_\delta + \frac{\xi_r}{\eta^2} \dot{n} - \frac{\omega_0 \xi_i}{2\eta^2} n = \frac{\Delta_i}{2\omega_0 E_0}, \quad (\text{A.8})$$

$$\dot{\phi} + \frac{\xi_i}{\eta^2} \dot{n} + \frac{\omega_0 \xi_r}{2\eta^2} n = -\frac{\Delta_r}{2\omega_0 E_0}, \quad (\text{A.9})$$

$$\dot{n} + \frac{n}{\tau_R} + \frac{2\eta^2 \omega_R^2}{\omega_0 \xi_i} E_\delta = \vartheta, \quad (\text{A.10})$$

$$\omega_R^2 = \frac{\epsilon_0 \omega_0 \chi_i(n_0) \xi_i E_0^2}{2\hbar \eta^2} = g(n_0) \left. \frac{dg}{dn} \right|_{n_0} p_0, \quad (\text{A.11})$$

$$\frac{1}{\tau_R} = \frac{1}{\tau_s} + \frac{\epsilon_0 \xi_i E_0^2}{2\hbar} = \frac{1}{\tau_s} + \left. \frac{dg}{dn} \right|_{n_0} p_0, \quad (\text{A.12})$$

where ξ_r and ξ_i are the first order coefficients of Taylor expansions of χ_r and χ_i near steady state n_0 . \ddot{E}_δ , $\ddot{\phi}$, $\dot{E}_\delta \dot{\phi}$ and \ddot{n} are neglected compared with the laser frequency ω_0 .

Appendix B. Langevin force coefficients

Langevin force relationships:

$$\langle \Delta_i(t + \tau) \Delta_i(t) \rangle = \langle \Delta_r(t + \tau) \Delta_r(t) \rangle = G \delta(\tau), \quad (\text{B.1})$$

$$\langle \Delta_i(t + \tau) \Delta_r(t) \rangle = \langle \Delta_r(t + \tau) \vartheta(t) \rangle = 0, \quad (\text{B.2})$$

$$\langle \Delta_i(t + \tau) \vartheta(t) \rangle = G_1 \delta(\tau), \quad (\text{B.3})$$

$$\langle \vartheta(t + \tau) \vartheta(t) \rangle = G_2 \delta(\tau), \quad (\text{B.4})$$

where $\delta(\tau)$ is the Dirac-delta function, G , G_1 , G_2 are the normalized coefficients.

The Langevin forces Δ_i and ϑ are [15]:

$$\Delta_i(t) = \frac{2\hbar \omega_0^3}{\epsilon_0 V E_0} \sum_n a_n \delta(t - t_n), \quad (\text{B.5})$$

$$\vartheta(t) = \frac{1}{V_c} \sum_n b_n \delta(t - t_n), \quad (\text{B.6})$$

where V and V_c are the mode volume and the carriers volume, a_n and b_n are 1 or -1 corresponding to accident emission or absorption. Therefore,

$$G = \frac{4\hbar \omega_0^3 E_{cv}}{\epsilon_0 V}, \quad (\text{B.7})$$

$$G_1 = -\frac{\omega_0 E_0}{V_c} (E_{cv} + E_{vc}), \quad (\text{B.8})$$

$$G_2 = \frac{p_0 V}{V_c^2} (E_{cv} + E_{vc}) + \frac{n_0}{V_c \tau_s}, \quad (\text{B.9})$$

where $E_{cv} p_0$ and $E_{vc} p_0$ are the stimulated emission and absorption rates per unit volume, respectively.

Appendix C. Lineshape formula in DSHO method

The electric field in DSHO method is:

$$\begin{aligned} E_O(t) = E_0 \exp[i(\omega_0 t + \phi(t))] \\ + E_0 \exp[i(\omega_0(t + \tau_d) + \phi(t + \tau_d))]. \end{aligned} \quad (\text{C.1})$$

Therefore, the autocorrelation function of photocurrent is

$$R(\tau) = \langle E_O(t + \tau) E_O^*(t + \tau) E_O(t) E_O^*(t) \rangle, \quad (\text{C.2})$$

$$= I_0 \exp \left[-\frac{1}{2} \langle [\Delta\phi(t + \tau_d, \tau) - \Delta\phi(t, \tau)]^2 \rangle \right]. \quad (\text{C.3})$$

Using the relation

$$\langle \phi^2(\tau) \rangle = \frac{1}{\pi} \int_{-\infty}^{\infty} W_f(\omega) \frac{1 - \cos(\omega\tau)}{\omega^2} d\omega, \quad (\text{C.4})$$

one can obtain

$$R_I(\tau) = I_0 \exp \left[-\frac{4}{\pi} \int_{-\infty}^{\infty} W_f(\omega) \times \frac{(1 - \cos \omega\tau)(1 - \cos \omega\tau_d)}{\omega^2} d\omega \right]. \quad (\text{C.5})$$

References

- [1] J.W. Kim, et al., *Appl. Opt.* 38 (1999) 1742.
- [2] P. Gysel, R.K. Staubli, *IEEE Photonics Technol. Lett.* 1 (1989) 327.
- [3] J.A. Constable, I.H. White, *Electron. Lett.* 30 (1994) 140.
- [4] H. Ludvigsen, M. Tossavainen, M. Kaivola, *Opt. Commun.* 155 (1998) 180.
- [5] A.L. Schawlow, C.H. Townes, *Phys. Rev.* 112 (1958) 1940.
- [6] C.H. Henry, *IEEE J. Quantum Electron.* 18 (1982) 259.
- [7] K. Vahala, A. Yariv, *IEEE J. Quantum Electron.* 19 (1983) 889.
- [8] L.E. Richter, et al., *IEEE J. Quantum Electron.* 22 (1986) 2070.
- [9] L.B. Mercer, *J. Lightwave Technol.* 9 (1991) 485.
- [10] K. Kikuchi, *IEEE J. Quantum Electron.* 25 (1989) 684.
- [11] A. Yariv, *Optical Electronics in Modern Communications*, fifth ed., Oxford Univ. Press, London, 1997.
- [12] U. Krüger, K. Petermann, *IEEE J. Quantum Electron.* 24 (1988) 2355.
- [13] F.C. Ndi, et al., *Proc. IEEE Conf. Opt. Fiber Commun.* 3 (2001) WDD25-1.
- [14] J.D. Jackson, *Classical Electrodynamics*, second ed., Wiley, New York, 1975.
- [15] K. Vahala, A. Yariv, *IEEE J. Quantum Electron.* 19 (1983) 1096.